Journal Name

ARTICLE

R-phycoerythrin extraction and purification from fresh *Gracilaria* sp. using thermo-responsive systems

Received 00th January 20xx,
Accepted 00th January 20xx

DOI: 10.1039/x0xx00000x

www.rsc.org/

Filipa A. Vicente[a], Inês S. Cardoso[a], Margarida Martins[a], Cátia V. M. Gonçalves[b], Ana C. R. V. Dias[b], Pedro Domingues[c], João A. P. Coutinho[a], Sónia P. M. Ventura[a,*]

R-phycoerythrin is a high added-value protein found in red macroalgae with several interesting properties. Despite the promissing results found when R-phycoerythrin is used as an optically active center in luminescent solar concentrators (LSCs), it still has some problems that can be attributed to the low stability of the R-phycoerythrin in presence of the specific contaminant proteins found in the crude extract. The development of downstream strategies able to reduce the use of environmentally hazardous solvents, while improving the purification without compromising the R-phycoerythrin structural integrity is still the biggest challenge to surpass. Aqueous micellar two-phase systems (AMTPS) appear as an appealing fractionation approach since they allow to process systems with larger water contents, while displaying great selectivity and biocompatibility with several biomolecules. Moroever, AMTPS that mix surfactants and surface-active ionic liquids are shown to significantly enhance the proteins purification. In this work, mixed AMTPS were applied to the R-phycoerythrin purification from red macroalgae. After the process optimization, this work proposes the application of two consecutive steps of purification as the final process to isolate R-phycoerythrin from the remaining proteins composing the crude extract, while keeping the R-phycoerythrin structural integrity, as requested to be used in the LSC. Besides a good performance, the two-step approach developed was also shown to have a lower environmental impact with a carbon footprint decrease of 16%, when compared with the conventional AMTPS.

Introduction

Red macroalgae (Rhodophyta) are marine natural raw materials rich in chemicals of economic/industrial interest. The algae coloration comes from the presence of three specific proteins, namely R-phycoerythrin, R-phycocyanin and allophycocyanin[1,2]. Phycobiliproteins act as photosynthetic pigments in Rhodophyta, with good stability from pH 4 to 10 and in temperatures up to 40°C.[3] These bioactive fluorescent compounds display a wide range of applications as probes, colorants, and nutraceuticals, due to their properties and biological activities, which explains their high commercial value.[4] Nowadays, their use address mainly the food, pharmaceutical, biomedical, and cosmetic fields.[4,5]

Recent works are addressing the development of innovative applications for the R-phycoerythrin, *e.g.*, in fluorescent-based detection systems[4] and as optically-active centers in luminescent solar concentrators (LSCs).[6,7] To meet the different purity demands (cosmetic, energy, pharmaceutical, just to mention a few), it is of utmost importance the development of a sustainable purification process to obtain R-phycoerythrin of enough purity, without compromising the structural integrity of the protein and its chromophores.

The most common industrial methodologies[4] describe the R-phycoerythrin purification by water leaching, staged precipitation with ammonium sulphate and ionic exchange chromatography (Patent CN 1587275A),[8] or by ammonium sulphate precipitation and ionic exchange chromatography (Patents CN 1271085C[9] and CN 101240009A,[10] differing only in the initial treatment of the sample). However, there is a worldwide demand to develop more cost-effective downstream processes for the most efficient purification of these fluorescent proteins from the aqueous crude extract.

Liquid-liquid extraction techniques appear as an attractive alternative, principally those based in aqueous two-phase systems (ATPS), consisting in the formation of two aqueous-rich immiscible phases formed by the mixture of two distinct phase formers, these being structurally different. Some examples are the combination of polymers, salts and/or ionic liquids (ILs) in water.[11,12] These are known for their high water content, sustainable nature and easy scale-up,[11] justifying their use on the purification of distinct compounds, from proteins and antibiotics to antibodies and dyes.[13] However, in spite of the good results reported,[13] the use of ATPS for the purification of some proteins does not yet allow us to reach the multi-product scenario envisaged under the scope of biorefinery.

Aqueous micellar two-phase systems (AMTPS) are a specific type of ATPS that has been explored in the last few years.[14,15] The poor interaction between the solvents of the AMTPS and the generality of the proteins[14,15] was the main criteria for their selection in this work.

[a] *CICECO, Departamento de Química, Universidade de Aveiro, 3810-193 Aveiro, Portugal.*
[b] *CESAM - Centre for Environmental and Marine Studies, Department of Environment and Planning, University of Aveiro, 3810-193 Aveiro, Portugal.*
[c] *Centro de Espectrometria de Massa, Departamento de Química & QOPNA, Departamento de Química, Universidade de Aveiro, 3810-193 Aveiro, Portugal.*

† Electronic Supplementary Information (ESI) available: [details of any supplementary information available should be included here]. See DOI: 10.1039/x0xx00000x

However, these systems, composed essentially of water and a surfactant, have the particularity of being thermo-responsive systems, *i.e.* it is the temperature change that induces the phase separation. For systems with a lower critical solution temperature (LCST), common to most of the nonionic surfactants, upon the temperature increase, the homogeneous system reaches a critical point, known as the cloud point, that corresponds to the specific temperature at which the solution becomes cloudy/turbid and the system coacervation occurs. The micelles coacervation induces a phase separation, creating two distinct environments: a hydrophobic surfactant-rich phase and a hydrophilic surfactant-poor phase. The determination of different cloud points as the surfactant concentration increases allows the determination of the system binodal curve, which represents the boundary between the monophasic and biphasic regions. This means that above the curve the system displays two phases, whereas upon a temperature decrease below the cloud point, the two macroscopic phases disappear as the system becomes homogeneous once again.[16] Although the development of systems with liquid-liquid immiscibility with an UCST or a LCST as thermo-responsive systems is a 'normal phenomenon' that upon heating above the critical (cloud) point, biphasic mixtures with a UCST become monophasic (or the opposite for biphasic mixtures with a LCST), this phase change can nevertheless be used with advantage for separation processes as previously shown by us and others.[14,17–19] These cloud points can be modified by the addition of inorganic salts, ionic surfactants, and surface-active ionic liquids (SAILs).[14,20] Several phase diagrams have recently been reported and characterized for a few nonionic surfactants belonging to the Tergitol family in presence and absence of SAILs.[20] Although being a 'normal phenomenon' this does not make them less simple to obtain as the extensive body of work attempting at creating compounds that present this behavior in aqueous solution, and the limited number of compounds that present critical points (UCST or LCST) in ranges of temperature that makes them useable for biomolecules purification making the development of these systems and processes based on them very challenging. Indeed, in addition to the SAILs influence on the cloud points, their incorporation into mixed micelles has also been proven to be helpful in enhancing the AMTPS extractive performance and selectivity.[14] While improving the selectivity and yields, AMTPS also allow a reduction of solvents, minimizing or precluding the use of environmentally hazardous solvents, thus improving the processes for a successful biorefinery approach.

This work started with the optimization of several process variables, namely the surfactant concentration, the equilibration time, the concentration of the phycobiliproteins crude extract added to the AMTPS, the pH and also the presence/absence of a pre-purification step using the ammonium sulphate precipitation. After selecting the most performant AMTPS and the best process conditions to separate the i) fluorescent from non-fluorescent proteins and the ii) R-phycoerythrin from R-phycocyanin, a complete process was investigated considering also the reuse of the solvents employed on the process. To evaluate the sustainability of this process, its environmental evaluation was carried considering the carbon footprint as the final output. In this analysis, the conventional AMTPS (*i.e.*, without the SAILs addition) and the mixed AMTPS (*i.e.*, in presence of the most performant SAIL in terms of purification) were the two scenarios studied.

Results and discussion

Solid-liquid extraction: characterization of phycobiliproteins crude extract

After the solid-liquid extraction, a crude extract rich in phycobiliproteins was obtained. A proteomic analysis was performed to characterize the different proteins present in the phycobiliproteins crude extract and their relative abundance, being the results depicted in Fig. 1 (and Table S3 of ESI). A representative nanoHPLC chromatogram of the injection of the tryptic digest of a SDS-PAGE spot, and a representative mass spectrum acquired during the run are also displayed in Fig. S1 of ESI. Accordingly to Fig.1, the proteins present in the crude extract can be divided into fluorescent (phycobiliproteins) and non-fluorescent. As fluorescent proteins, *Gracilaria* sp. has in its composition R-phycoerythrin, the most abundant phycobiliprotein, R-phycocyanin and allophycocyanin. Regarding the non-fluorescent proteins, the crude extract contains mostly ribulose bisphosphate carboxylase and ribulose-1,5-bisphosphate carboxylase/oxygenase small subunit, being the remaining proteins, detailed in Table S3 of ESI, included in the fraction Others of Fig. 1.

Purification of phycobiliproteins and R-phycoerythrin

Taking into account the characterization of the crude extract previously performed, the presence of contaminants demands the development of a purification process, in which contaminants and fluorescent proteins are separated. In this work, thermo-responsive AMTPS were used. Proteins are thermolabile biomolecules, and as such, their purification must consider this limitation, especially when thermo-responsive systems are used. The non-ionic surfactant Tergitol 15-S-7 was selected due to its low cloud point, ranging between 34 and 40°C (*cf.* Fig. S2), and which can be further controlled by the proper choice of a SAIL acting as a co-surfactant.[20] Besides, these mixed AMTPS have shown enhanced selectivity when compared with the AMTPS without any SAIL.[14] Thus, these systems seem promising for the purification of phycobiliproteins, in particular, R-phycoerythrin, from the red macroalgae *Gracilaria* sp., which is stable until 40°C.[3]

For the Tergitol 15-S-7/McIlvaine buffer-based AMTPS, the purification conditions were optimized considering the highest recovery of fluorescent and non-fluorescent proteins in the surfactant-poor and -rich phases, respectively, which in turn leads to highest selectivity, promoting as well, a decrease of the R-phycoerythrin contamination with R-phycocyanin. These results are shown in Figs. 2 and S3 to S9 of ESI. Herein, all studies were buffered with the McIlvaine buffer (pH 7.0), since it has been proved to provide an enhanced extraction of phycobiliproteins, while allowing R-phycoerythrin to maintain its structural integrity.[2] The surfactant concentration was the first parameter optimized, as shown in Fig.2.

Journal Name

ARTICLE

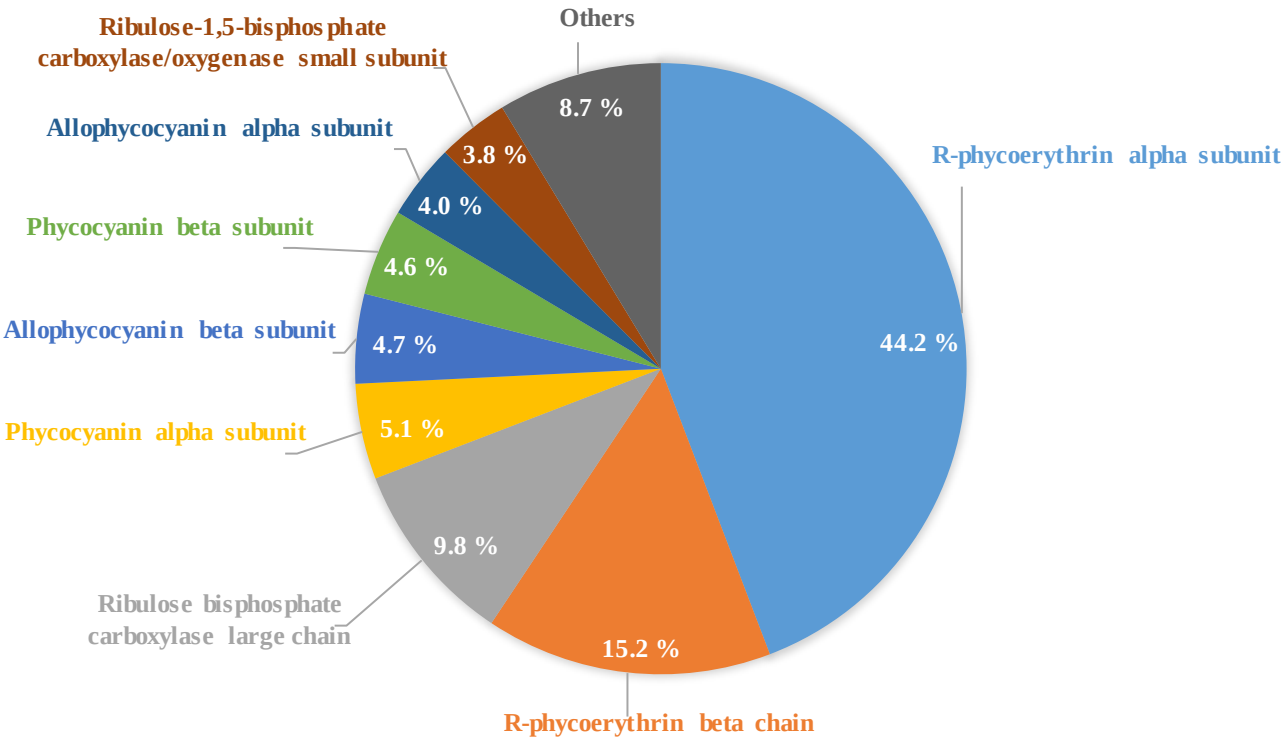

Fig. 1. Proteomic characterization of the phycobiliproteins crude extract obtained after the solid-liquid extraction with distilled water and used in this work. The proteins relative abundance (%) is also shown in the figure.

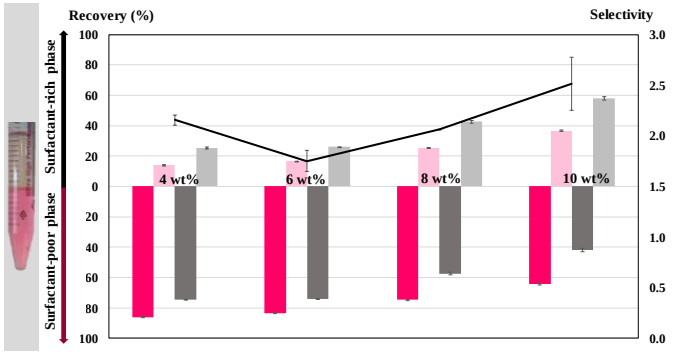

Fig. 2 Surfactant concentration effect upon the recovery of R-phycoerythrin and total proteins towards the surfactant-rich and -poor phases: ■ and ■, R-phycoerythrin recovery (%) in the surfactant-poor and surfactant-rich phases, respectively; ■ and ■, total proteins recovery (%) in the surfactant-poor and surfactant-rich phases, respectively. The line represents the selectivity.

The bars represent the recovery of phycobiliproteins (pink bars) and total proteins (grey bars) in both phases while the line corresponds to the selectivity parameter. These results suggest that the fluorescent phycobiliproteins and particularly R-phycoerythrin partitioned preferably towards the (most hydrophilic) surfactant-poor phase as shown by the recoveries (> 60%) and the pink color of the system's bottom phase (shown in Fig. 2) characteristic of the R-phycoerythrin presence. In contrast, the total proteins recovery in the surfactant-rich phase increases with the surfactant concentration, resulting in an increased selectivity trend as well. Additionally, there is also a decreased R-phycoerythrin contamination with R-phycocyanin as the surfactant concentration is increased (cf. Fig. S3 of ESI), thus justifying the selection of 10 wt% as the most performant surfactant concentration, being this kept constant during the subsequent optimization. Attempting at reducing the typical overnight extraction, the extraction time was evaluated, revealing that 3 h were enough for the phycobiliproteins partition between the two phases to reach the thermodynamic equilibrium. Yet, total proteins required 4 h to reach the partition equilibrium, so this time was selected for the next steps. After selecting the surfactant concentration and equilibration time, the effects of the extract concentration and system pH were tested. The results showed that, by increasing the concentration of phycobiliproteins extract, the system complexity was also increased, resulting in a lower extraction of total proteins into the surfactant-

rich phase. Thereby, it is preferable to use less extract if it means increasing the R-phycoerythrin purity in the lowest number of steps. Regarding the pH effect on the purification of the fluorescent proteins, it was evidenced that the system selectivity was the highest at neutral pH. Moreover, it was proved that an additional step of ammonium precipitation is not needed, since the results in its presence/absence were very similar.

A multi-product strategy requires the separation of the contaminant proteins present in the crude extract obtained in the first step of (solid-liquid) extraction. After optimizing the preliminary processual conditions considering the AMTPS use, a complete purification process able to separate (i) the fluorescent and non-fluorescent proteins and to isolate (ii) R-phycoerythrin from R-phycocyanin, was developed. For that purpose, thermo-responsive AMTPS based on Tergitol 15-S-7 with SAILs as co-surfactants were used, and the purification of phycobiliproteins, more precisely R-phycoerythrin, evaluated using the selectivity and R-phycocyanin contamination index as main parameters. A screening was performed using SAILs from distinct families, namely imidazolium, phosphonium, quaternary ammonium, pyridinium, cholinium and alkyl sulfonates, as presented in Fig. 3. These were selected not only because the mechanisms of formation of the two-phases were already understood, but also because their cloud points were in the range of temperatures in which the phycobiliproteins, and particularly the R-phycoerythrin, are thermostable.

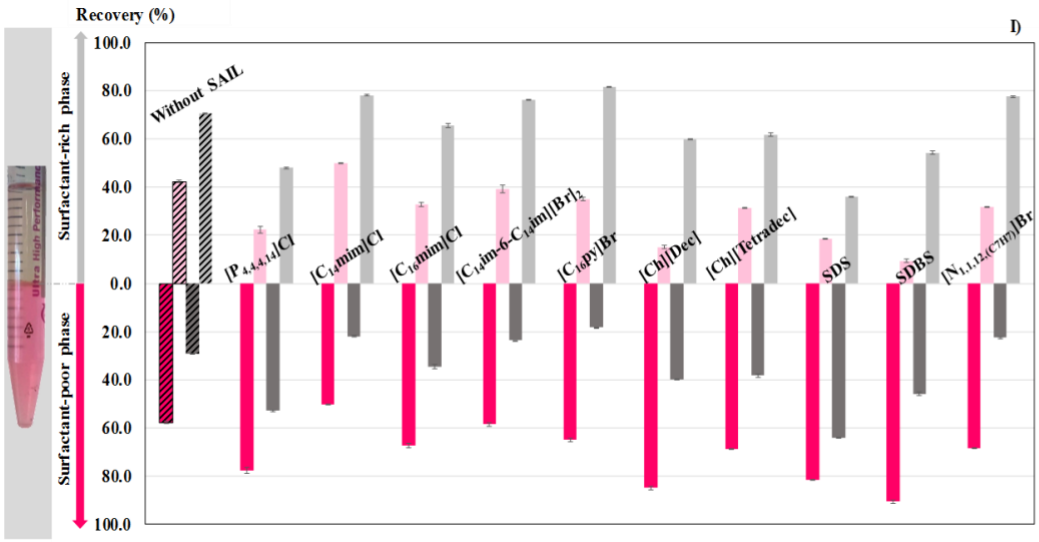

II)

AMTPS	Selectivity
SDS	2.51 ± 0.02
[P4,4,4,14]Cl	3.1 ± 0.3
Without SAIL	3.28 ± 0.08
[Ch][Tetradec]	3.53 ± 0.07
[C14mim]Cl	3.61 ± 0.05
[C16mim]Cl	3.91 ± 0.02
[C14Im-6-C14Im][Br]2	4.76 ± 0.09
[Ch][Dec]	7.4 ± 0.2
SDBS	7.4 ± 0.4
[N1,1,12,(C7H7)]Br	7.5 ± 0.1
[C16py]Cl	7.6 ± 0.2

Fig. 3. Extractive performance of distinct AMTPS in absence and presence of SAILs using the mixture point composed of 10 wt% of Tergitol 15-S-7 + 0 or 0.3 wt% of SAIL + 10 wt% of phycobiliproteins extract + 80 or 79.7 wt% of McIlvaine buffer pH 7.0: I) ■ and ■, R-phycoerythrin recovery (%) in the surfactant-poor and surfactant-rich phases, respectively; ■ and ■, total proteins recovery (%) in the surfactant-poor and surfactant-rich phases, respectively. The Table represented in the inset II) shows the alues of selctivity obtained for each AMTPS under study.

The R-phycoerythrin (pink bars) and total proteins (grey bars) recovery results in both phases as well as the selectivity (table) were the parameters determined. The results suggest that, apart from the [C_{14}mim]Cl-based AMTPS, all the mixed AMTPS were able to increase the R-phycoerythrin recovery in the surfactant-poor phase while recovering identical or higher amounts of total proteins in the surfactant-rich phase, hence, increasing the selectivity of the system. If fixing our analysis in the selectivity results (Fig.3.II), it seems that only the mixed AMTPS composed of SDS showed a lower selectivity (S = 2.51 ± 0.02) than the system without SAILs, while the [$P_{4,4,4,14}$]Cl-based AMTPS displayed a similar selectivity (S = 3.1 ± 0.3) to this non-additivated AMTPS (S = 3.28 ± 0.08). The remaining mixed AMTPS improved the R-phycoerythrin purification according to the following sequence: SDS < [$P_{4,4,4,14}$]Cl ≈ without SAIL < [Ch][Tetradec] ≈ [C_{14}mim]Cl < [C_{16}mim]Cl < [C_{14}im-6-C_{14}im]Br_2 < [Ch][Dec] ≈ SDBS < [$N_{1,1,12,(C7H7)}$]Br ≈ [C_{16}py]Br. This suggests that the R-phycoerythrin purification is independently of the IL family under study since very distinct results were observed within the quaternary ammonium family, for instance. Here, [Ch][Dec] and [$N_{1,1,12,(C7H7)}$]Br showed outstanding results compared with the average results attained with [Ch][Tetradec]. Therefore, the different characteristics and properties of the mixed micelles being formed, and/or the establishment of more specific interaction should be dictating the proteins partitioning. Regarding the R-phycoerythrin contamination with R-phycocyanin (Fig. 4), there is only one system that does not display any contamination: the AMTPS based in [$N_{1,1,12,(C7H7)}$]Br, which may be justified by the different sizes of both phycobiliproteins or even by some specific interactions taking place between the micelles formed and the contaminant fluorescent protein. Indeed, the contamination with R-phycocyanin follows a different trend than the one obtained for the selectivity: [$N_{1,1,12,(C7H7)}$]Br < [C_{14}mim]Cl < [Ch][Dec] ≈ [C_{16}py]Br ≈ SDS < without SAIL < SDBS < [C_{14}im-6-C_{14}im]Br_2 < [$P_{4,4,4,14}$]Cl < [C_{16}mim]Cl < [Ch][Tetradec]. In these systems, the purification is normally dependent upon the hydrophobicity/hydrophilicity of the biomolecules and the micelles size.[21]

Journal Name

ARTICLE

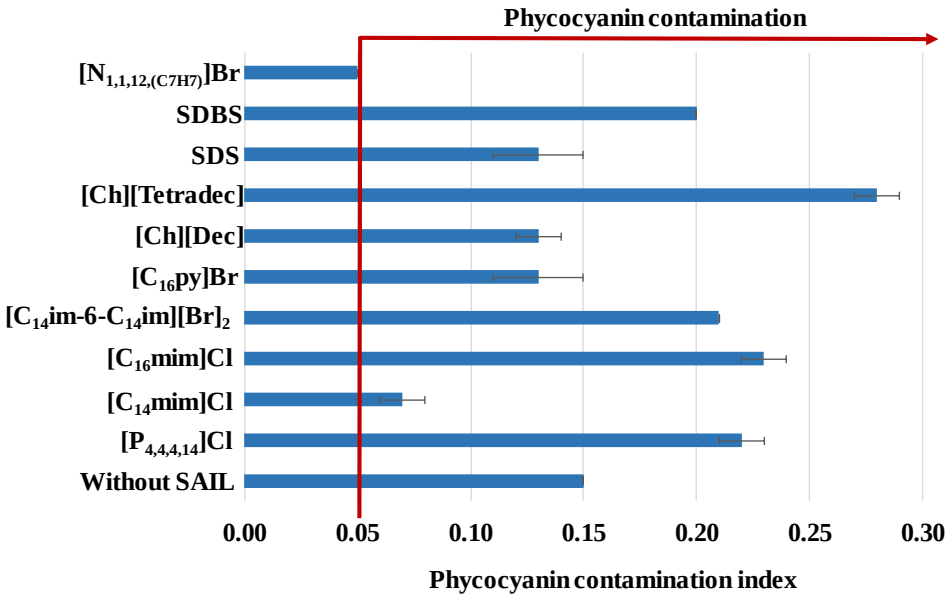

Fig. 4. Phycocyanin contamination index of AMTPS in absence and presence of SAILs, using the mixture point composed of 10 wt% of Tergitol 15-S-7 + 0 or 0.3 wt% of SAIL + 10 wt% of phycobiliproteins extract + 80 or 79.7 wt% of McIlvaine buffer pH 7.0.

Taking this into account, it would be assumed that the systems displaying micelles with larger diameters should be the ones inducing a higher purification since they might extract a higher amount of contaminants. However, it is not here the case. As recently shown by us,[20] SDBS and [Ch][Tetradec] are, from the SAILs studied in this work, those inducing the formation of the largest micelles (between 40 and 50 nm) when compared with the 7-8 nm of the remaining mixed AMTPS and the ~14 nm of the micelles obtained for the non-additivated AMTPS. The results here obtained show a higher purification performance for the AMTPS with lower micelle diameter, which might suggest, once again, that interactions between the proteins and the micelles, rather than the micelles size, may be controlling the partitions observed.

Complete process using sequential AMTPS steps

For some applications of R-phycoerythrin a high purity degree is required. To achieve higher purity levels, sequential steps of purification were used. To optimize this process, the recovery of R-phycoerythrin and total proteins, the selectivity, and the R-phycocyanin contamination index were the parameters considered (Table 1). The most promising systems selected from the SAILs screening were tested, namely the mixed AMTPS composed of [C_{16}py]Br, [Ch][Dec], SDBS and [$N_{1,1,12,(C7H7)}$]Br. The non-additivated AMTPS was used once again as reference. It should be noticed that due to its high selectivity and ability to isolate R-phycoerythrin from R-phycocyanin, the [$N_{1,1,12,(C7H7)}$]Br was always used as co-surfactant in the second purification step.

The goal behind the development of this process was the separation of phycobiliproteins from the non-fluorescent proteins in the first step and then, the purification of R-phycoerythrin from the R-phycocyanin, in the second step. Table 1 shows very similar results regarding the recovery of R-phycoerythrin towards the surfactant-poor phase in both steps. On the other hand, the recovery of total proteins on the surfactant-poor phase tends to decrease in all systems with the second step, except for the [C_{16}py]Br-based AMTPS used in the first step. In this system, the replacement of the SAIL in the second step seems to induce a higher partition of both fluorescent and non-fluorescent proteins towards the bottom phase, thus reducing the process purification performance. Overall, a purification trend of these systems can be established as follows: [C_{16}py]Br/[$N_{1,1,12,(C7H7)}$]Br < without SAIL/[$N_{1,1,12,(C7H7)}$]Br ≈ [Ch][Dec]/[$N_{1,1,12,(C7H7)}$]Br < SDBS/[$N_{1,1,12,(C7H7)}$]Br < [$N_{1,1,12,(C7H7)}$]Br/[$N_{1,1,12,(C7H7)}$]Br. These results clearly show an enhanced performance of the mixed systems compared to the traditional one (without any SAIL). Moreover, the proper manipulation of the AMTPS is also driving the selectivity of the systems, which was more than doubled (maximum S = 13.6 ± 0.1)

when compared with the non-additivated AMTPS (S = 5.86 ± 0.04). Concerning the R-phycoerythrin contamination with R-phycocyanin (Table 1), the results evidence that the $[N_{1,1,12,(C7H7)}]Br$ addition to all systems considerably reduces this contamination. Unexpectedly, the first step of the $[N_{1,1,12,(C7H7)}]Br$-based AMTPS presented some contamination with R-phycocyanin, probably as a result of the algae heterogeneity (due to the weather and daylight length and intensity).[22] The cells heterogeneity results in significant amounts of R-phycocyanin being extracted from the cells and, consequently, present in the phycobiliproteins-rich extract used in the complete process. Nevertheless, this was overcome in the second step. The seaweed heterogeneity also affected the selectivity, leading to an overall selectivity reduction. Yet, the same tendency was followed.

Table 1. R-phycoerythrin and total proteins recovery in the surfactant-rich and -poor phases, their selectivity, and R-phycocyanin contamination index for the first and second steps of the process.

Cycle of purification	System	Recovery (%)				Selectivity	R-phycocyanin contamination index
		R-phycoerythrin		Total proteins			
		Top phase	Bot phase	Top phase	Bot phase		
1st step	Without SAIL	17.4 ± 0.4	82.6 ± 0.4	55.0 ± 0.8	45.0 ± 0.8	5.9 ± 0.3	0.16 ± 0.01
2nd step	$[N_{1,1,12,(C7H7)}]Br$	15.3 ± 0.9	84.7 ± 0.8	59 ± 1	41 ± 1	5.86 ± 0.04	0.13 ± 0.01
1st step	$[C_{16}py]Br$	25 ± 1	77 ± 1	71.4 ± 0.3	28.7 ± 0.3	8.0 ± 0.8	0.28 ± 0.03
2nd step	$[N_{1,1,12,(C7H7)}]Br$	16.4 ± 0.3	83.6 ± 0.3	59 ± 1	41 ± 1	5.4 ± 0.3	0.18 ± 0.01
1st step	[Ch][Dec]	19 ± 2	81 ± 2	58.6 ± 0.5	41.4 ± 0.5	6.0 ± 0.8	0.13 ± 0.01
2nd step	$[N_{1,1,12,(C7H7)}]Br$	15.4 ± 0.9	84.7 ± 0.8	59 ± 1	41 ± 1	6.1 ± 0.3	0.12 ± 0.01
1st step	SDBS	10 ± 1	89 ± 1	40 ± 1	55 ± 1	7.1 ± 0.6	0.147 ± 0.004
2nd step	$[N_{1,1,12,(C7H7)}]Br$	22 ± 1	80 ± 1	64 ± 6	30 ± 6	7 ± 1	0.07 ± 0.02
1st step	$[N_{1,1,12,(C7H7)}]Br$	25 ± 3	77 ± 3	71.4 ± 0.9	28.7 ± 0.9	8.00 ± 0.02	0.10 ± 0.01
2nd step	$[N_{1,1,12,(C7H7)}]Br$	25.2 ± 0.8	78.8 ± 0.8	82.1 ± 0.5	17.9 ± 0.5	13.60 ± 0.09	0.047 ± 0.004

Summing up, a process using two AMTPS extraction steps was developed and efficiently implemented as an effective downstream process to isolate R-phycoerythrin. However, and foreseeing its industrial implementation, the recycling and reuse of the main solvents are essential steps. The complete process proposed is shown in Fig. 5, in which three main steps were included. The process starts with the conventional solid-liquid extraction of phycobiliproteins using water. Then, the aqueous extract rich in phycobiliproteins proceeds to the two purification steps, in which AMTPS based in SAILs were sequentially applied. During the first AMTPS step, it was possible to retain ~77% of R-phycoerythrin into the surfactant-poor phase and extract *circa* of 71% of total proteins, including most of contaminant non-fluorescent proteins, into the opposite phase. The surfactant-poor phase was then fed to a second AMTPS step, allowing a further R-phycoerythrin purification by removal of the R-phycocyanin, retaining ~79% of it in the new surfactant-poor phase. From the remaining ~29% of total proteins that were still in first surfactant-poor phase, it was possible to extract ~82%, which considerably improved the R-phycoerythrin purity. Moreover, in the schematic diagram of the process, the isolation step used to separate the surfactant-rich phase from proteins was experimentally tested since this was required to finish the process regarding the reuse of the major part of the surfactant. Here, the surfactant-rich phase, containing most of the system phase formers (surfactant and SAIL), was submitted to a precipitation with cold acetone used to precipitate the contaminant proteins. FTIR spectra of both the resuspended pellet containing the precipitated proteins and the acetone supernatant containing the phase formers were acquired. The results indicate that all the tensioactive agents were completely removed from the contaminant proteins (*cf.* Fig. S10 of ESI). Afterwards, a distillation step can be introduced to separate the acetone from the surfactant, allowing the recovery of both components to be further applied in a new cycle. Meanwhile, the use of ultrafiltration[23–25] is pointed out as a strategy to separate the surfactant-poor phase from the R-phycoerythrin. In this work, this step was only envisaged theoretically, since this task will be only needed for some specific final applications of R-phycoerythrin, a scenario not further explored in this work. Finally, the stability and structural integrity of R-phycoerythrin were analysed.

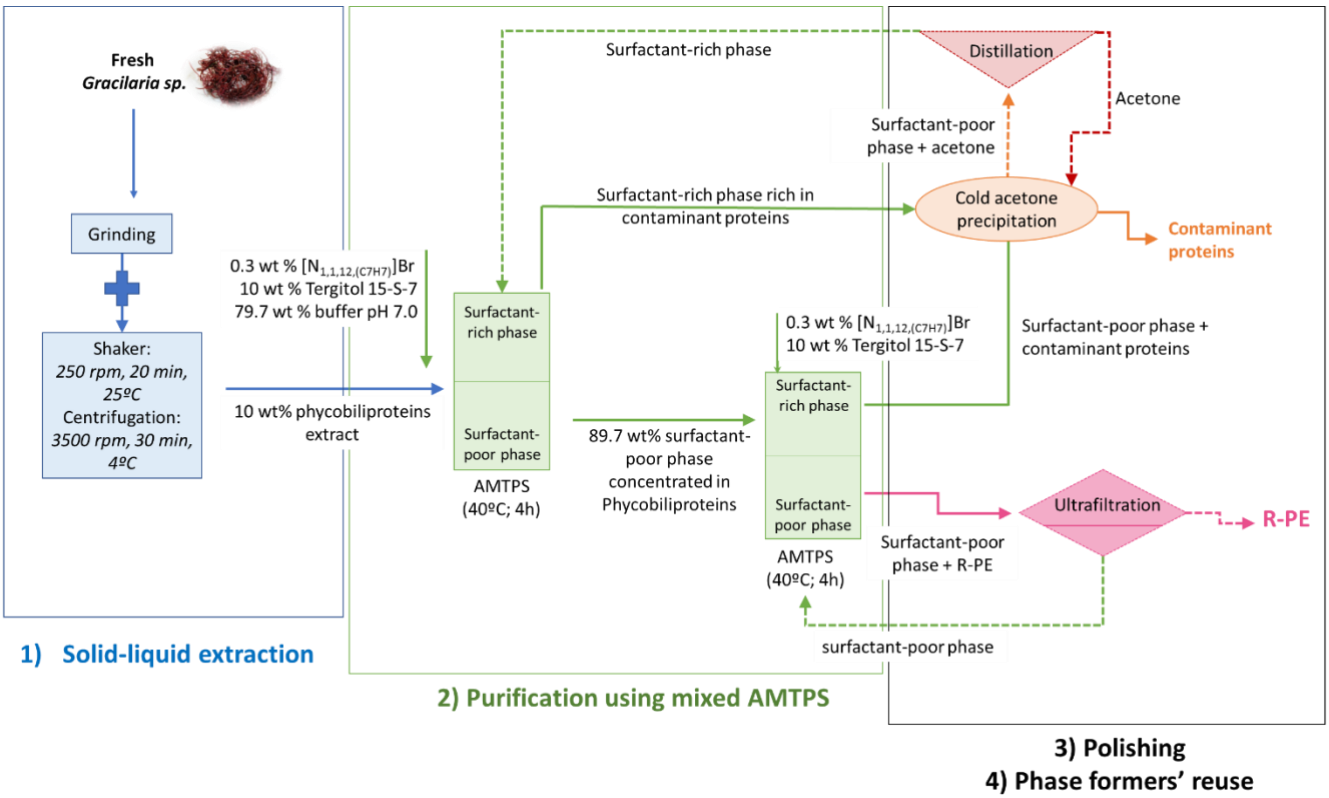

Fig. 5. Diagram of the complete process developed to purify R-phycoerythrin (but also phycobiliproteins). The proposed approach considers the use of two steps of purification by applying mixed AMTPS based in $[N_{1,1,12,(C7H7)}]Br$ as co-surfactant. The polishing of R-phycoerythrin and the recycling and reuse of the main phase formers is theoretically described. Note: the part described with a dashed line was not performed experimentally.

Circular dichroism is one of the most used techniques to infer about the structural integrity of proteins by analysing their secondary structure, namely their content in α-helix, β-sheet, β-turn and random coils. This is possible by analysing the spectrum in the range of 240 nm and below, aiming at identifying the peptide bonds.[26] The macroalgae crude extract was analysed and compared to the spectra of the most selective AMTPS ($[N_{1,1,12,(C7H7)}]Br$) and the non-additivated system, after both steps, to conclude about the stability of R-phycoerythrin. This was possible through the direct comparison between our data and the R-phycoerythrin analysis found elsewhere,[2] where it was shown that the secondary structure of pure R-phycoerythrin presents more than 70% of α-helix. In this context, all samples were diluted until a good spectrum was obtained, and the spectra were normalized before the data analysis (Fig. 6). This data shows that the crude extract is mostly composed of α-helix due to the negative bands at 210 and 220 nm and the positive band below 200 nm, just like pure R-phycoerythrin. The spectra show that, during the complete purification process, the proteins can maintain their integrity, since these bands are kept in all AMTPS spectra after both purification steps.

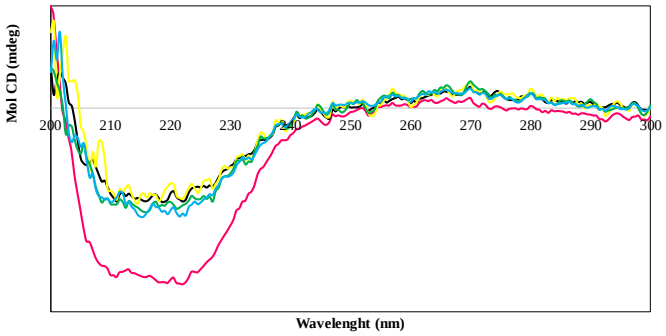

Fig. 6. Circular dichroism analysis of the R-phycoerythrin stability after two consecutive steps of purification from the macroalgae crude extract: –, crude extract; –, without SAIL (1st step); – , without SAIL/$[N_{1,1,12,(C7H7)}]Br$, – , $[N_{1,1,12,(C7H7)}]Br$ (1st step); – , $[N_{1,1,12,(C7H7)}]Br/[N_{1,1,12,(C7H7)}]Br$.

Environmental evaluation

To evaluate the sustainability of the process here proposed, which included the steps of extraction and purification of R-PE, an environmental evaluation was carried considering the carbon footprint as the main output. Both scenarios proposed, namely the application of a conventional AMTPS and the most performant mixed AMTPS (using $[N_{1,1,12(C7H7)}]Br$ as co-surfactant) for R-phycoerythrin purification were addressed, being the main results obtained shown in Fig. 6. The carbon footprint is 81.30 kg $CO_{2\ eq}.mg^{-1}_{R\text{-}phycoerythrin}$ when the conventional AMTPS (1st step) + mixed AMTPS (2nd step) and decreases in 16% the GHG emissions when the mixed AMTPS is used in both steps (carbon footprint = 68.14 kg $CO_{2\ eq}.mg^{-1}_{R\text{-}phycoerythrin}$). The steps of polishing and phase formers reuse were not taken into account in this analysis and, therefore, the carbon footprint of the production of acetone and energy consumed in these steps was not considered. Besides, possible emissions of acetone to air would not be accounted for in the carbon footprint, since acetone is not a greenhouse gas.

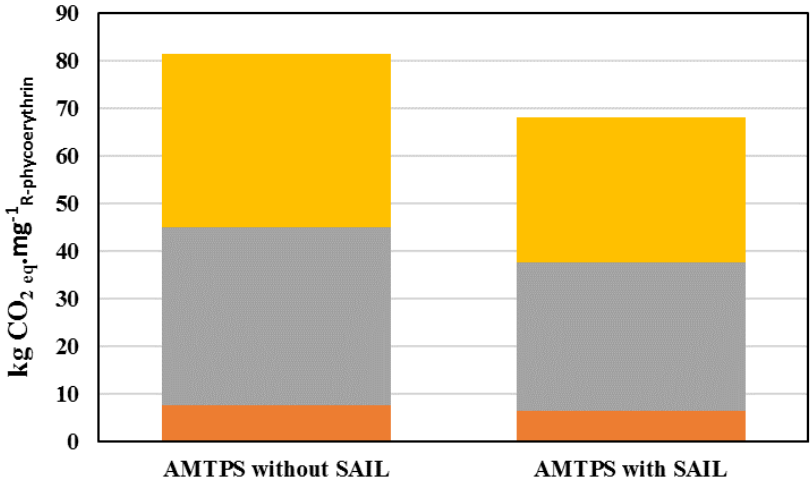

Fig. 7. Carbon footprint for the two scenarios considered: i) conventional AMTPS in the first liquid-liquid extraction and with the addition of $[N_{1,1,12,(C7H7)}]Br$ in the second liquid-liquid extraction, ii) AMTPS with $[N_{1,1,12,(C7H7)}]Br$ in both extractions. Results are expressed kg $CO_{2eq}.mg^{-1}_{R\text{-}phycoerythrin}$ purified: ■, algae preparation, ■, solid-liquid extraction, ■, 1st liquid-liquid extraction, and ■, 2nd liquid-liquid extraction.

The main contribution to the carbon footprint in both scenarios comes mainly from the energy consumption (first and the second liquid-liquid extraction steps, respectively 46% and 45% of the total). The energy consumption to promote the phase separation in these two stages, represents almost 90% of the total carbon footprint. A comparison of the results achieved in this work is not possible, considering not only the lack of published data on the carbon footprint evaluation but also due to the lack of similar processes. Summing up, if in one hand, the extraction efficiency of the process increases, on the other hand, the GHG emissions associated with the application of mixed AMTPS to purify R-phycoerythrin are lowered.

Conclusions

R-phycoerythrin purification was successfully achieved in this study by using thermo-responsive systems. Results show the recovery of most phycobiliproteins in the surfactant-poor phase whereas most non-fluorescent (contaminant) proteins were collected in the surfactant-rich phase. The mixed AMTPS have proven to be more selective than the non-additivated system, being the best results achieved with two consecutive steps of the $[N_{1,1,12,(C7H7)}]Br$-based AMTPS. This system was not only able to isolate the R-phycoerythrin from the remaining proteins composing the initial crude aqueous extract while maintaining its structural integrity, but it also allowed the recycle and reuse of the surfactant through an ultrafiltration process that could be easily implemented at an industrial level. The carbon footprint of the complete process was evaluated (*per* mass of R-phycoerythrin) and found to decrease 16% when the mixed AMTPS was applied instead of the non-additivated one. Herein, it was demonstrated that the presence of $[N_{1,1,12,(C7H7)}]Br$ increases the efficiency of the system, while GHG emissions for the same algae content remain almost the same. The results obtained on this work demonstrate the applicability and advantages of mixed AMTPS using SAILs as co-surfactants.

Experimental

Materials

The non-ionic surfactant Tergitol 15-S-7 (purity ≥ 99%) was acquired at Sigma-Aldrich as well as the hexadecylpyridinium bromide – $[C_{16}py]Br$ (purity = 97.0%), benzyldodecyldimethylammonium bromide - $[N_{1,1,12,(C7H7)}]Br$ (purity > 99%) and sodium dodecylbenzenesulfonate, SDBS (technical grade). The imidazolium-based SAILs, 1-tetradecyl-3-methylimidazolium chloride, $[C_{14}mim]Cl$ (purity > 98%) and 1-hexadecyl-3-methylimidazolium chloride, $[C_{16}mim]Cl$ (purity > 98%) were purchased from Iolitec (Ionic Liquid Technologies, Heilbronn, Germany), while 3-(1-tetradecyl-3-hexylimidazolium)-1-tetradecylimidazolium dibromide $[C_{14}im\text{-}6\text{-}C_{14}im]Br_2$ was synthesized in-house using well established procedures.[27] The same protocol was used to synthetize

cholinium decanoate, [Ch][Dec] and cholinium tetradecanoate, [Ch][Tetradec]. The phosphonium-based SAIL tributyltetradecylphosphonium chloride, $[P_{4,4,4,14}]Cl$ (purity = 97.1%) was kindly offered by Cytec. Sodium dodecylsulphate, SDS (purity = 99%) was supplied by Acros Organics. These structures are presented in Fig. 8. McIlvaine buffer (0.18 M) constituted by citric acid monohydrate $C_6H_8O_7 \bullet H_2O$ (purity ≥ 99%) was used in all systems, and sodium phosphate dibasic heptahydrate $Na_2HPO_4 \bullet 7H_2O$ (purity ≥ 99%), both acquired from Panreac AppliChem.

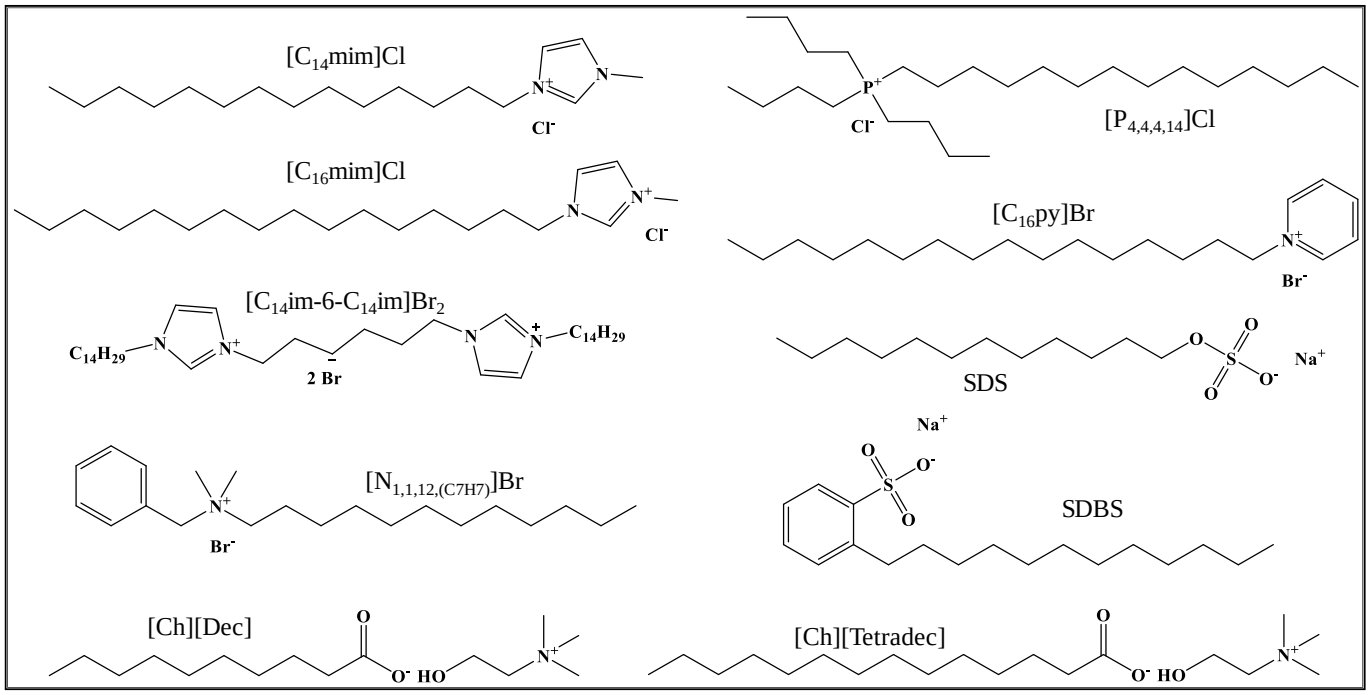

Fig. 8. Chemical structure of SAILs added as co-surfactants in the AMTPS used to purify phycobiliproteins.

Methods

Solid-liquid extraction of phycobiliproteins. Fresh *Gracilaria* sp. was cultivated by ALGAplus Ltda, a Portuguese company specialized in the Integrated Multi-Trophic Aquaculture (IMTA) production of marine macroalgae, located in Ílhavo, Portugal. Macroalgae samples were collected from aquaculture between April and November of 2016, and in January of 2017. After collecting the macroalgae, the samples were cleaned and washed with fresh and distilled water at least 3 times, weighted and stored in a freezer at -20°C pending further use.

Algae samples were previously grounded while frozen with liquid nitrogen, homogenized in distilled water (with a solid-liquid ratio of 0.7) at room temperature and placed in an incubator shaker (IKA KS 4000 ic control) for 20 min, at 250 rpm and room temperature. During the solid-liquid extraction step, all samples were protected from light exposure due to the high light sensitivity of phycobiliproteins. Then, the solution was filtered and, subsequently, the filtrate originated was centrifuged in a Thermo Scientific Heraeus Megafuge 16 R Centrifuge at 3500 rpm for 30 min, at 4°C. The resultant pellet was discarded, and the phycobiliproteins-rich supernatant was collected (phycobiliproteins crude extract) for further purification studies.

SDS-PAGE procedure. The phycobiliproteins crude extract was analysed through an electrophoresis that was prepared on polyacrylamide gels (stacking: 4% and resolving: 20%) with a running buffer consisting of 250 mM of Tris HCl, 1.92 M of glycine, and 1% of SDS. The proteins were stained with the usual staining procedure [Coomassie Brilliant Blue G-250 0.1% (w/v), methanol 50% (v/v), acetic 7% (v/v), and water 42.9% (v/v)] in an orbital shaker, at moderate speed, for 2-3 hours at room temperature. The gels were distained in a solution containing acetic acid 7% (v/v), methanol 20% (v/v), and water 73% (v/v) in an orbital shaker at a moderate speed (± 60 rpm) during 3-4 hours at room temperature. SDS-PAGE Molecular Weight Standards, Marker molecular weight full-range (VWR), were used as protein standards. All gels were analysed using the Image Lab 3.0 (BIO-RAD) analysis tool.

Extract analysis by proteomics. Tryptic digestion was performed according to,[28] with a few modifications. Protein spots were manually excised from the gel and transferred to Eppendorf tubes. The gel spots were washed with 25 mM ammonium bicarbonate/50% acetonitrile and then with acetonitrile. Gel pieces were dried in a SpeedVac (Thermo Savant) and rehydrated in digestion buffer containing 12.5 $\mu g.mL^{-1}$ sequence grade modified porcine trypsin (Promega) in 25 mM ammonium bicarbonate. 100 µL of 25 mM ammonium bicarbonate were then added and the samples were incubated overnight at 37°C. Extraction of tryptic peptides was performed by the addition of 10% formic acid/50% acetonitrile three times. Tryptic peptides were lyophilized in a SpeedVac (Thermo Savant) and resuspended in 5% acetonitrile/0.1% formic acid

solution. The samples were analysed with a QExactive Orbitrap (Thermo Fisher Scientific, Bremen) that was coupled to an Ultimate 3000 (Dionex, Sunnyvale, CA) HPLC (high-pressure liquid chromatography) system. The trap (5 mm × 300 µm I.D.) and analytical (150 mm × 75 µm I.D.) columns used were C18 Pepmap100 (Dionex, LC Packings). Peptides were trapped at 30 µL.min^{-1} in 95% solvent A (0.1 % formic acid/5% acetonitrile v/v). Elution was achieved with the solvent B (0.1 % formic acid/100% acetonitrile v/v) at 300 nL.min^{-1}. The 50 min gradient used was as follows: 0–3 min, 95% solvent A; 3–21 min, 5–45% solvent B; 21–35 min, 45–90% solvent B; 35–37 min, 90% solvent B; 37–40 min, 10–95% solvent A; 40–50 min, 95% solvent A. The mass spectrometer was operated in the data dependent acquisition mode. A MS2 method was used with a FT survey scan from 400 to 1600 m/z (resolution 70,000; AGC target 1E6). The 10 most intense peaks were subjected to HCD fragmentation (resolution 17,500; AGC target 5E4, NCE 28%, max. injection time 60 ms, dynamic exclusion 35 s). General mass spectrometer parameters were: Nano electrospray voltage, 1.8 kV; no sheath and auxiliary gas flow; ion transfer tube temperature, 275 °C; S-lens RF level 60.0. Spectra were processed and analysed using Proteome Discoverer (version 2.2, Thermo), with the MS Amanda (version 2.0, University of Applied Sciences Upper Austria, Research Institute of Molecular Pathology) and the SequestHT search engines. Uniprot Swiss-Prot protein sequence database (version of June 2018) was used for all searches under *Gracilaria* (genus). Database search parameters were as follows: carbamidomethylation and carboxymethyl of cysteine as a variable modification as well as oxidation of methionine, and the allowance for up to two missed tryptic cleavages. The peptide mass tolerance was 10 ppm and fragment ion mass tolerance was 0.05 Da. To achieve a 1% false discovery rate, the Percolator (version 2.2, Thermo) node was implemented for a decoy database search strategy, peptides were filtered for high confidence and a minimum length of 6 amino acids, minimum of two peptides and proteins were filtered for only rank 1 peptides. The average of intensities of the three most intense peptide ions was used to generate relative quantitative data.

Purification of phycobiliproteins using AMTPS. For the phycobiliproteins purification using AMTPS, falcon tubes were weighed with specific amounts of each component: 10 wt% of phycobiliproteins crude extract, 10 wt% of surfactant and 0 or 0.3 wt% of SAIL, being the system completed with McIlvaine buffer (0.18 M) pH 7.0 up to a final volume of 10 mL. The systems were homogenized around 2 h using a tube rotator apparatus model 270 from Fanem, at 40 rpm. Then, the tubes were left in a temperature above the cloud point of the systems (40°C) for 4 h, allowing the thermodynamic equilibrium to be reached, resulting in the formation of the surfactant-rich (top) and a surfactant-poor (bottom) phases. Both phases were carefully separated, and their volumes and weight composition measured. Then, the quantification of both phycobiliproteins and total proteins was assessed for each phase, by UV spectroscopy (Molecular Device Spectramax 384 Plus | UV-Vis Microplate Reader) at 565 nm and 280 nm, respectively. The analytical quantifications were performed in triplicate. Blank controls, *i.e.*, identical systems without the phycobiliproteins extract, were performed for each system to eliminate any possible interference of the phase formers upon the quantification. The concentration of R-phycoerythrin and total proteins in the extracts was assessed according to calibration curves previously determined in the same UV-Vis equipment.

In this work, the purification performance of each AMTPS was analysed through the Partition coefficient, Recovery, and Selectivity. The Contamination index was also determined to investigate the elimination of R-phycocyanin contamination from R-phycoerythrin. The partition coefficient ($K_{R\text{-phycoerythrin}}$) was calculated as the ratio between the amount of R-phycoerythrin present in the surfactant-poor (bottom) and the surfactant-rich (top) phases, as described by Eq. 1. The partition coefficient of total proteins ($K_{total\ proteins}$) was determined identically (Eq. 2).

$$K_{R-phycoerythrin} = \frac{[R-phycoerythrin]_{bot}}{[R-phycoerythrin]_{top}} \qquad \text{(Eq. 1)}$$

$$K_{total\ proteins} = \frac{[total\ proteins]_{bot}}{[total\ proteins]_{top}} \qquad \text{(Eq. 2)}$$

where $[\text{R-phycoerythrin}]_{bot}$ and $[\text{R-phycoerythrin}]_{top}$ are, respectively, the concentration of R-phycoerythrin (in mg.mL^{-1}) in the bottom and top phases; and $[\text{total proteins}]_{bot}$ and $[\text{total proteins}]_{top}$ are the total proteins concentration (in mg.mL^{-1}) in the bottom and top phases, respectively. The recovery (R) parameter of R-phycoerythrin and the total protein content towards the bottom (R_{bot}) and top (R_{top}) phases were determined following Eqs. 3 and 4, respectively:

$$R_{bot} = \frac{100}{1+\left(\frac{1}{R_v \times K}\right)} \qquad \text{(Eq. 3)}$$

$$R_{top} = \frac{100}{1+ R_v+K} \qquad \text{(Eq. 4)}$$

where R_v stands for the ratio between the volumes of the bottom and top phases. Finally, the selectivity ($S_{R-phycoerythrin/total\ proteins}$) of the AMTPS herein applied was described as indicated by Eq. 5:

$$S_{R-phycoerythrin/total\ proteins} = \frac{K_{R-phycoerythrin}}{K_{total\ proteins}} \qquad \text{(Eq. 5)}$$

The phycocyanin contamination index (Eq. 6) was determined by the ratio between the absorbance at 620 nm and 565 nm, which belongs to the R-phycocyanin and R-phycoerythrin wavelengths, respectively. For ratios lower than 0.05, it is considered that no significant contamination by R-phycocyanin is found, as previously described in literature.[3]

$$Phycocyanin\ contamination\ index = \frac{Abs_{620}}{Abs_{565}} \quad \text{(Eq. 6)}$$

Purification of R-phycoerythrin using consecutive extractions. To increase the R-phycoerythrin purification, the surfactant-poor phase was reused for a second step. The first step was carried out as previously described but this time for a total of 25 g. Here, only the SAILs that led to the highest selectivity for the elimination of the contaminant non-fluorescent proteins were used. The second step was carried out by adding 10 wt% of Tergitol 15-S-7 + 0.3 wt% of the selected SAIL + 89.7 wt% of the surfactant-poor phase of the first AMTPS, up to a total of 10 g.

Study of the stability of R-phycoerythrin. To guarantee that, at the end of the purification, the R-phycoerythrin maintains its structural integrity, circular dichroism (CD) measurements were used to evaluate the protein secondary structure. The surfactant-poor phases of (i) the conventional AMTPS (*i.e.*, without SAIL) and (ii) the best SAIL-based AMTPS were analysed using CD spectroscopy (JASCO-1500). The spectra were collected in a 1 mm path length quartz cuvette at a scan rate of 100 nm per minute, at 20°C cell temperature. The response time and the bandwidth were 2 seconds and 0.2 nm, respectively. Three spectra were recorded consecutively to give single average data.

Environmental evaluation: Carbon footprint analysis. The environmental evaluation was carried out taking into account two scenarios for R-phycoerythrin purification, namely by using (i) the conventional system, where the AMTPS is used in the absence of SAIL as co-surfactant, and (ii) the mixed AMTPS, with the presence of the most promising SAIL selected.

The environmental assessment of the two systems chosen was performed by calculating the carbon footprint as output. This indicator is the sum of greenhouse gas (GHG) emissions expressed as carbon dioxide equivalent (CO_2 eq) from a life cycle perspective. The carbon footprint allows quantifying various GHG emissions associated with the two different systems tested and identifying their main causes.

This analysis includes the production of all reagents (McIlvaine buffer, non-ionic surfactant Tergitol 15-S-7, and SAIL selected), and other consumables (tap and distilled water, and liquid nitrogen), besides the electricity consumed by the equipment used throughout the different processes.

Data on the amount of reagents, tap and distilled water, liquid nitrogen and electricity consumed were obtained during the experiment and from equipment catalogs (Table S1). Data on GHG emissions from the production of reagents, liquid nitrogen and electricity were sourced from Ecoinvent database version 3.4[29] and are present in Table S2. The GHG emissions for the production of distilled water were calculated based on GHG emissions from tap water production[30] and GHG emissions from electricity consumption during the distillation process. All data refer to 5 g of *Gracilaria* sp.

Conflicts of interest

There are no conflicts to declare.

Acknowledgements

This work was developed within the scope of the project CICECO-Aveiro Institute of Materials, FCT Ref. UID/CTM/50011/2019, financed by national funds through the FCT/MCTES, CESAM (UID/AMB/50017 - POCI-01-0145-FEDER-007638), and QOPNA research unit (FCT UID/QUI/00062/2013) financed by national funds through the FCT/MEC and when appropriate co-financed by FEDER under the PT2020 Partnership Agreement. It was also supported by the Integrated Programme of SR&TD "SusPhotoSolutions - Soluções Fotovoltaicas Sustentáveis" (reference CENTRO-01-0145-FEDER-000005), co-funded by Centro 2020 program, Portugal 2020, European Union, through the European Regional Development Fund. The authors are grateful for the national fund through the Portuguese Foundation for Science and Technology (FCT) for the doctoral grants SFRH/BD/101683/2014 of F.A. Vicente and SFRH/BD/122220/2016 of M. Martins. S.P.M. Ventura and A.C.R.V. Dias acknowledges FCT for the contracts IF/00402/2015 and IF/00587/2013, respectively. Thanks are also due to Fundação para a Ciência e a Tecnologia (FCT, Portugal), for funding RNEM (REDE/1504/REM/2005) the Portuguese Mass Spectrometry Network.

Notes and references

1 S. M. A. Kawsar, Y. Fujii, R. Matsumoto, H. Yasumitsu and Y. Ozeki, *Phytol. Balc.*, 2011, **17**, 347 – 354.

2 M. Martins, F. A. Vieira, I. Correia, R. A. S. Ferreira, H. Abreu, J. A. P. Coutinho and S. P. M. Ventura, *Green Chem.*, 2016, **18**, 63–68.

3 M. Munier, S. Jubeau, A. Wijaya, M. Morançais, J. Dumay, L. Marchal, P. Jaouen and J. Fleurence, *Food Chem.*, 2014, **150**, 400–407.

4 S. Sekar and M. Chandramohan, *J. Appl. Phycol.*, 2008, **20**, 113–136.

5 R. R. Sonani, R. P. Rastogi, R. Patel and D. Madamwar, *World J. Biol. Chem.*, 2016, **7**, 100–9.

6 J. Ihssen, A. Braun, G. Faccio, K. Gajda-Schrantz and L. Thöny-Meyer, *Curr. Protein Pept. Sci.*, 2014, **15**, 374–84.

7 J. Ma, H. Chen and S. Q. and H. Lin, *Curr. Biotechnol.*, 2015, **4**, 275–281.

8 P. CN 1587275A, 2004.

9 P. CN 1271085C, 2005.

10 P. CN 101240009A, 2008.

11 M. G. Freire, A. F. M. Cláudio, J. M. M. Araújo, J. A. P. Coutinho, I. M. Marrucho, J. N. Canongia Lopes and L. P. N. Rebelo, *Chem. Soc. Rev.*, 2012, **41**, 4966–95.

12 S. P. M. Ventura, F. A. e Silva, M. V Quental, D. Mondal, M. G. Freire and J. A. P. Coutinho, *Chem. Rev.*, 2017, **117**, 6984–7052.

13 J. V. D. Molino, D. de A. Viana Marques, A. P. Júnior, P. G. Mazzola and M. S. V. Gatti, *Biotechnol. Prog.*, 2013, **29**,

1343–1353.
14 F. A. Vicente, L. P. Malpiedi, F. A. e Silva, A. P. Jr., J. A. P. Coutinho and S. P. M. Ventura, *Sep. Purif. Technol.*, 2014, **135**, 259–267.
15 F. A. Vicente, L. D. Lario, A. Pessoa Jr. and S. P. M. Ventura, *Process Biochem.*, 2015, **51**, 528–534.
16 B. Kronberg, K. Holmberg and B. Lindman, *Surface Chemistry of Surfactants and Polymers*, Wiley, 2014.
17 H. Passos, A. Luís, J. A. P. Coutinho and M. G. Freire, *Sci. Rep.*, 2016, **6**, 20276.
18 K. Ikeda, R. Ikari, N. Nakamura, H. Ohno and K. Fujita, *J. Electrochem. Soc.*, 2018, **165**, G96–G100.
19 A. M. Ferreira, H. Passos, A. Okafuji, A. P. M. Tavares, H. Ohno, M. G. Freire and J. A. P. Coutinho, *Green Chem.*, 2018, **20**, 1218–1223.
20 F. A. Vicente, I. S. Cardoso, T. E. Sintra, J. Lemus, E. F. Marques, S. P. M. Ventura and J. A. P. Coutinho, *J. Phys. Chem. B*, 2017, **121**, 8742–8755.
21 C.-L. Liu, Y. J. Nikas and D. Blankschtein, *Biotechnol. Bioeng.*, 1996, **52**, 185–192.
22 C. A. de Oliveira, W. de Castro Oliveira and S. M. Rocha, *Eur. J. Biol. Med. Sci. Res.*, 2014, **2**, 23–36.
23 C. Denis, A. Massé, J. Fleurence and P. Jaouen, *Sep. Purif. Technol.*, 2009, **69**, 37–42.
24 J. H. P. M. Santos, G. Carretero, J. A. P. Coutinho, C. O. Rangel-Yagui and S. P. M. Ventura, *Green Chem.*, 2017, **19**, 5800–5808.
25 J. H. P. M. Santos, M. R. Almeida, C. I. R. Martins, A. C. R. V Dias, M. G. Freire, J. A. P. Coutinho and S. P. M. Ventura, *Green Chem.*, 2018, **20**, 1906–1916.
26 S. M. Kelly, T. J. Jess and N. C. Price, *Biochim. Biophys. Acta - Proteins Proteomics*, 2005, **1751**, 119–139.
27 T. E. Sintra, M. Vilas, M. Martins, S. P. M. Ventura, A. I. M. C. L. Ferreira, L. M. N. B. F. Santos, F. Gonçalves, E. Tojo and J. A. P. Coutinho, *ACS Sust Chem Eng, Submitt.*
28 A. Shevchenko, H. Tomas, J. Havli, J. V Olsen and M. Mann, *Nat. Protoc.*, 2007, **1**, 2856.
29 Ecoinvent, http://www.ecoinvent.org.
30 D. Lemos, A. C. Dias, X. Gabarrell and L. Arroja, *J. Clean. Prod.*, 2013, **54**, 157–165.

